Chapter II : Theory

2.1 Introduction

The fiber Bragg grating (FBG) is a periodic perturbation of the refractive index n(z) along the fiber length. The FBG characteristics can be understood and modeled by several approaches [1~5]. Coupled mode theory is often the fundamental for many of these computations. The most distinguishing feature of FBGs is the flexibility they offer for achieving desired spectral characteristics. Numerous physical parameters can be varied, including: induced index change, length, apodization, period chirp, fringe tilt, and whether the grating supports counter propagating or co-propagating coupling at a desired wavelength. By varying these parameters, a grating can be made with normalized bandwidths ($\Delta\lambda/\lambda$) between $0.1 \sim 10^{-4}$, extremely sharp spectral features, and tailorable dispersion characteristics. In this chapter, we focus on the optical properties of the short period FBG. In section 2.2, we examine the properties of uniform gratings when coupling occurs between two counter propagation modes, since this case yields simple solutions for reflection and transmission. In section 2.3, the analysis is extended to include two-modes coupling in non-uniform gratings such as apodized and chirped gratings.

FBGs are produced by exposing an optical fiber to a spatially varying pattern of ultraviolet intensity. The result is a perturbation to the effective index n_{eff} of the guided mode of interest, described by

$$\delta n_{eff}(z) = \overline{\delta n}_{eff}(z)\{1 + \upsilon \cos[\frac{2\pi}{\Lambda} z + \phi(z)]\} \tag{2.1}$$

where $\overline{\delta n}_{eff}$ is the "dc" index change spatially averaged over a grating period, υ is the fringe visibility of the index change, Λ is the nominal period, and $\phi(z)$ describes grating chirp. If the induced index change is a linear function of the intensity of the interference laser beams, the visibility υ is constrained to lie between 0 (no grating) and 1 (perfectly balanced interferometer). Figure 2.1 illustrates the variation of the induced index change along the fiber axis for some common types of FBGs. For illustrative purpose the size of the grating period relative to grating length has been greatly exaggerated.

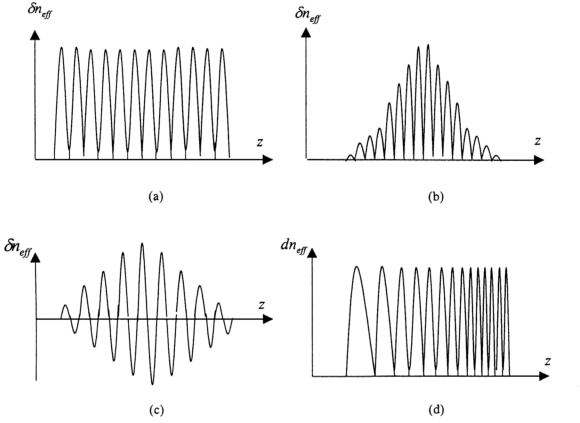

Figure 2.1: Index modulation in common FBGs (a) uniform (b) Gaussian-apodized (c) raised-cosine apodized (d) chirped

2.2 Resonant wavelength for grating diffraction

A FBG is simply an optical diffraction grating and thus its effect upon a light wave incident on the grating at an angle θ_1 can be described by the familiar grating equation [6]

$$n\sin\theta_2 = n\sin\theta_1 + m(\lambda/\Lambda) \tag{2.2}$$

where θ_2 is the angle of the diffracted wave and the integer m determines the diffracted order (see Figure 2.2). This equation predicts the directions θ_2 into which constructive interference occurs and also capable of determining the wavelength at which a fiber grating most efficiently couples light between two modes.

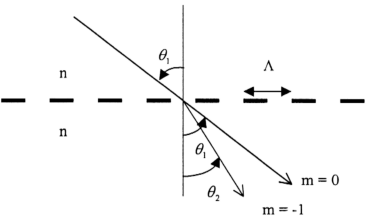

Figure 2.2: The diffraction of a light wave by a grating

In FBGs (also called short period gratings), a coupling occurs between modes traveling in opposite directions. Figure 2.2 illustrates reflection by a Bragg grating of a mode with a bounce angle of θ_1 into the same mode travelling in the opposite direction with a bounce angle of $\theta_2 = -\theta_1$. Since the mode propagation constant β where it is simply $(2\pi/\lambda)n_{eff}$ and $n_{eff} = n_{co}\sin\theta$, we may rewrite equation (2.2) for guided modes as

$$\beta_2 = \beta_1 + m(2\pi / \Lambda) \tag{2.3}$$

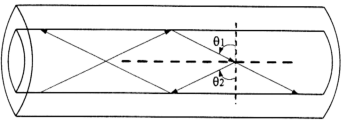

Figure 2.3: Ray-optic illustration of core-mode Bragg reflection by a fiber Bragg grating

For first order diffraction, which usually dominates in a Bragg grating, m = -1. By using equation (2.3) and recognizing $\beta_2 < 0$ (negative values describe modes that propagate in the –z direction), we find that the resonant wavelength for reflection of a mode of index $n_{eff,1}$ into a mode of index $n_{eff,2}$ is

$$\lambda = (n_{eff,1} + n_{eff,2})\Lambda \tag{2.4}$$

If the two modes are identical, we get the familiar result for Bragg reflection: $\lambda_B = 2n_{eff}\Lambda$.

2.3 Coupled mode theory

Coupled mode theory is a good tool for obtaining quantitative information about the diffraction efficiency and spectral dependence of fiber gratings. It's straightforward, intuitive and capable of modeling accurately the optical properties of most fiber gratings of interest. The derivations of coupled mode theory are detailed in numerous articles and texts [7], [8]. In the ideal mode approximation to coupled mode theory, it is assumed that the transverse component of the electric field can be written as a superposition of the ideal modes labeled j (i.e., the modes with no grating perturbation), such that

$$\vec{E}_t(x,y,z,t) = \sum_j [A_j(z)\exp(i\beta_j z) + B_j(z)\exp(-i\beta_j z)].\vec{e}_{jt}(x,y)\exp(-i\omega t) \qquad (2.5)$$

where A_j *(z)* and B_j *(z)* are slowly varying amplitudes of the *j*th mode traveling in the $+z$ and $-z$ directions, respectively. The transverse mode fields $\vec{e}_{jt}(x,y)$ might describe cladding modes. The modes are orthogonal and do not exchange energy in an ideal waveguide, but the perturbation causes the modes to be coupled such that the amplitudes A_j and B_j of the jth mode evolve along the z axis according to

$$\frac{dA_j}{dz} = i\sum_k A_k(K_{kj}^t + K_{kj}^z)\exp[i(\beta_k - \beta_j)z]$$

$$+ i\sum_k B_k(K_{kj}^t - K_{kj}^z)\exp[-i(\beta_k + \beta_j)z] \qquad (2.6)$$

$$\frac{dB_j}{dz} = -i\sum_k A_k(K_{kj}^t - K_{kj}^z)\exp[i(\beta_k + \beta_j)z]$$

$$- i\sum_k B_k(K_{kj}^t + K_{kj}^z)\exp[-i(\beta_k - \beta_j)z] \qquad (2.7)$$

In equations (2.6) and (2.7), K_{kj}^t *(z)* is the transverse coupling coefficient between modes *j* and *k* given by

$$K_{kj}^t(z) = \frac{\omega}{4}\iint_{\infty} dxdy\ \Delta\varepsilon\ (x,y,z)\ \vec{e}_{kt}(x,y)\ .\ \vec{e}^{\,*}_{jt}(x,y) \qquad (2.8)$$

where $\Delta\varepsilon$ is the perturbation of the permittivity, approximately $\Delta\varepsilon \cong 2n\delta n$ when $\delta n << n$. The longitudinal coefficient K_{kj}^z *(z)* is analogous to K_{kj}^t *(z)*, but generally K_{kj}^z *(z)* << K_{kj}^t *(z)* for fiber modes, and thus this coefficient is usually neglected.

The induced index change $\delta n(x,y,z)$ in most of gratings is approximately uniform across the core and nonexistent outside the core. We can thus describe the

core index by an expression similar to equation (2.1), but with replacing $\overline{\delta n}_{eff}(z)$ to $\overline{\delta n}_{co}(z)$. We define two new coefficients

$$\sigma_{kj}(z) = (\omega n_{co}/2)\overline{\delta n}_{co}(z) \iint_{core} dxdy \ \vec{e}_{kt}(x,y) \cdot \vec{e}^{\,*}_{jt}(x,y) \tag{2.9}$$

$$\kappa_{kj}(z) = \frac{v}{2}\sigma_{kj}(z) \tag{2.10}$$

where σ is a "dc" (period averaged) coupling coefficient and κ is an "AC" coupling coefficient. Then, we can thus write the general coupling coefficient as

$$K^{l}_{kj}(z) = \sigma_{kj}(z) + 2\kappa_{kj}(z)\cos\left[\frac{2\pi}{\Lambda}z + \phi(z)\right] \tag{2.11}$$

Equations (2.6) ~ (2.11) are the coupled-mode equations that can be used to describe FBG spectra below.

2.4 Fiber Bragg gratings

The interaction between a mode of amplitude *A(z)* and an identical counter-propagating mode of amplitude *B(z)* is the dominant interaction in uniform FBGs. Equations (2.6) and (2.7) are the coupled mode equation from which the transfer characteristics of the Bragg grating can be calculated. To find a solution, the following substitutions are made for the forward (reference) and backward propagating (signal) modes [9] :

$$R(z) \equiv A(z)\ exp\ (\ i\delta z - \phi/2\ ) \tag{2.12}$$

$$S(z) \equiv B(z)\ exp\ (-\ i\delta z + \phi/2\ ) \tag{2.13}$$

Differentiation of equations (2.12) and (2.13) result in the following equations,

$$\frac{dR}{dz} = i\hat{\sigma}\,R(z) + i\kappa S(z) \tag{2.14}$$

$$\frac{dS}{dz} = -i\hat{\sigma}S(z) - i\kappa^{*}R(z) \tag{2.15}$$

where κ is the "AC" coupling coefficient from equation (2.10) and $\hat{\sigma}$ is a general "dc" self coupling coefficient defined as

$$\hat{\sigma} \equiv \sigma + \delta - \frac{1}{2}\frac{d\phi}{dz} \tag{2.16}$$

The σ is the "dc" coupling coefficient which influences propagation due to the change in the average refractive index of the mode and is defined as

$$\sigma = \frac{2\pi}{\lambda}\overline{\delta n}_{eff} \quad . \tag{2.17}$$

Any absorption, scattering loss, or gain can be incorporated in the magnitude and sign of the imaginary part of σ. δ is the detuning which indicates how rapidly the power is exchanged between the radiated field and polarization field, is defined to be

$$\begin{aligned} \delta &\equiv \beta - \frac{\pi}{\Lambda} \\ &= \beta - \beta_D \\ &= 2\pi n_{eff}\left(\frac{1}{\lambda} - \frac{1}{\lambda_D}\right) \end{aligned} \tag{2.18}$$

where λ_D is the "design wavelength" for Bragg scattering. At phase matching, when $\delta = 0$, we find $\lambda_D \equiv 2n_{eff}\Lambda$, the field couples to the generated wave over an infinite distance. Finally, the rate of change of ϕ signifies a chirp in the period of the grating and has an effect similar to that of the detuning. So, for a uniform grating $\overline{\delta n}_{eff}$ is a constant, $\frac{d\phi}{dz} = 0$, and thus κ, σ and $\hat{\sigma}$ are constants.

Equations (2.14) and (2.15) are coupled first-order ordinary differential equations with constant coefficients, for which closed-form solution can be found

when appropriate boundary conditions are specified. The reflectivity of a uniform fiber grating (of length L) can be found by assuming that the amplitude of the incident wave from -∝ at the input of a grating at $z = -L/2$ is $R(-L/2) = 1$ and that the field $S(L/2) = 0$. The latter condition is satisfied by the fact that the reflected field at the output end of the grating cannot exist owing to the absence of the perturbation beyond that region. The amplitude and power reflection coefficients $\rho = S(-L/2)/R(L/2)$ and $r = |\rho|^2$, respectively, can then be shown to be [7], [8]

$$\rho = \frac{-\kappa \sinh(\alpha L)}{\hat{\sigma}\sinh(\alpha L) + i\alpha \cosh(\alpha L)} \tag{2.19}$$

and

$$r = \frac{\sinh^2(\alpha L)}{\cosh^2(\alpha L) - \frac{\hat{\sigma}^2}{\kappa^2}} \tag{2.20}$$

where

$$\alpha = \sqrt{\kappa^2 - \hat{\sigma}^2} \quad . \tag{2.21}$$

A number of interesting features of FBGs can be seen from these results. For the purpose of illustration, Figure 2.4 shows the power reflectivity r of two Bragg grating with different coupling constants κL of 2 and 8, plotted versus the normalized wavelength

$$\frac{\lambda}{\lambda_{max}} = \frac{1}{1 + \frac{\hat{\sigma}L}{\pi N}} \tag{2.22}$$

where N is the total number of grating period ($N=L/\Lambda$) and λ_{max} is the wavelength at which maximum reflectivity occurs. If N were larger or smaller, the reflectivity bandwidth would be narrower or broader, respectively, for a given value of κL. From equation (2.20), we find the maximum reflectivity r_{max} for a Bragg grating is

$$r_{max} = tanh^2(\kappa L) \tag{2.23}$$

and it occurs when $\hat{\sigma}$ =0, or at the wavelength

$$\lambda_{max} = (1 + \frac{\overline{\delta n}_{eff}}{n_{eff}})\lambda_D \tag{2.24}$$

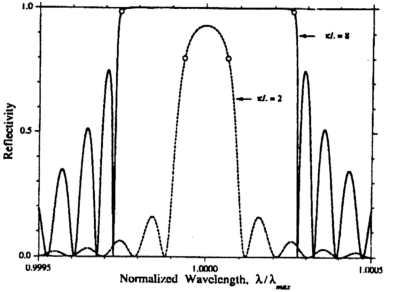

Figure 2.4: Reflection spectrum versus normalized wavelength for uniform FBG [10].

The points on Figure 2.4 denoted by open circles indicate the "band edges," or the points at the edges of the "band gap"; defined such that $|\hat{\sigma}| < \kappa$. Inside the band gap, the amplitudes *R(z)* and *S(z)* grow and decay exponentially along z. The reflectivity at the band edges is

$$r_{bandedge} = \frac{(\kappa L)^2}{1+(\kappa L)^2} \tag{2.25}$$

and the band edges occur at the wavelengths

$$\lambda_{bandedge} = \lambda_{max} \pm \frac{\nu \overline{\delta n}_{eff}}{2n_{eff}} \lambda_D . \tag{2.26}$$

From (2.26) the normalized bandwidth of a Bragg grating as measured at the band edges is simply

$$\frac{\Delta\lambda_{bandedge}}{\lambda} = \frac{\nu\overline{\delta n}_{eff}}{n_{eff}} \tag{2.27}$$

where $\nu\overline{\delta n}_{eff}$ is simply the "AC" part of the induced index change.

A more readily measurable bandwidth for a uniform Bragg grating is that between the first zeros of either side of the maximum reflectivity. Looking at the excursion of $\hat{\sigma}$ from $\hat{\sigma} = 0$ that causes the numerator in (2.20) to go to zero, we find

$$\frac{\Delta\lambda_0}{\lambda} = \frac{\nu\overline{\delta n}_{eff}}{n_{eff}} \sqrt{1 + (\frac{\lambda_D}{\nu\overline{\delta n}_{eff} L})^2}. \tag{2.28}$$

In the "weak-grating limit," for which $\nu\overline{\delta n}_{eff}$ is very small, we find

$$\frac{\Delta\lambda_0}{\lambda} \rightarrow \frac{\lambda_D}{n_{eff} L} = \frac{2}{N} \qquad (\nu\overline{\delta n}_{eff} << \frac{\lambda_D}{L}) \tag{2.29}$$

the bandwidth of weak grating is said to be "length-limited." However, in the "strong-grating limit," we find

$$\frac{\Delta\lambda_0}{\lambda} \rightarrow \frac{\nu\overline{\delta n}_{eff}}{n_{eff}} \qquad (\nu\overline{\delta n}_{eff} >> \frac{\lambda_D}{L}) \ . \tag{2.30}$$

In strong gratings, the light does not penetrate the full length of grating, and thus the bandwidth is independent of length and directly proportional to the induced index change. For strong gratings the bandwidth is similar whether measured at the band edges, at the first zeros, or as the full-width-at-half-maximum (FWHM).

The group delay and dispersion of the reflected light can be determined from the phase of the amplitude reflection coefficient ρ in (2.19). If we denote $\theta_\rho \equiv phase\ (\rho)$, then at a local frequency ω_0 we may expand θ_ρ in a Taylor series about ω_0.

Since the first derivation $d\theta_\rho / d\omega$ is directly proportional to the frequency ω, this quantity can be identified as a time delay. Thus, the time delay τ_ρ for reflected light from a grating is

$$\tau_\rho = \frac{d\theta_\rho}{d\omega} = - \frac{\lambda^2}{2\pi c} \frac{d\theta_\rho}{d\lambda} . \tag{2.31}$$

τ_ρ is usually given in units of picoseconds. Figure 2.5 shows the delay τ_ρ calculated from the two example gratings from Figure 2.4. Here the grating length is L = 1cm, the design wavelength is λ_D = 1550nm, n_{eff} =1.45, and the fringe visibility is υ = 1. For the weaker grating in Figure 2.5(a), $\overline{\delta n}_{eff}$ = 1 x 10^{-4} , while for the stronger grating in Figure 2.5(b), $\overline{\delta n}_{eff}$ = 4 x 10^{-4} . We see that for unchirped uniform gratings both the reflectivity and the delay are symmetric about the wavelength λ_{max} .

Since the dispersion d_ρ (in ps/nm) is the rate of change in delay with wavelength, we find

$$\begin{aligned} d_\rho &= \frac{d\tau_\rho}{d\lambda} \\ &= \frac{2\tau_\rho}{\lambda} - \frac{\lambda^2}{2\pi c} \frac{d^2\theta_\rho}{d\lambda^2} \\ &= - \frac{2\pi c}{\lambda^2} \frac{d^2\theta_\rho}{d\omega^2} \end{aligned} \tag{2.32}$$

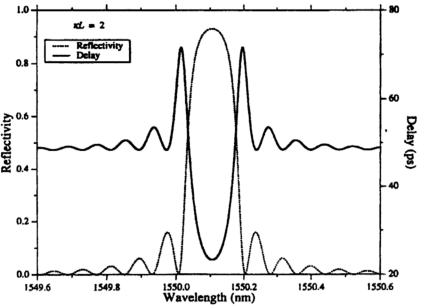

(a) $\kappa L = 2$

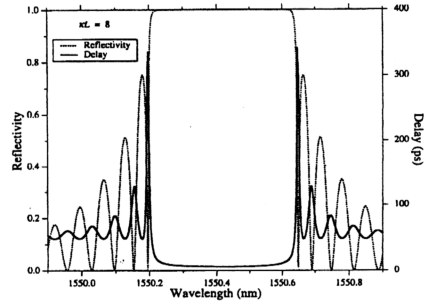

(b) $\kappa L = 8$

Figure 2.5: Calculated reflection spectrum (dotted line) and group delay (solid line) for uniform FBG with (a) $\kappa L = 2$ (b) $\kappa L = 8$ [10].

In a uniform grating, the dispersion is zero near λ_{max}, and only becomes appreciable near the band edges and side lobes of the reflection spectrum, where it tends to vary rapidly with wavelength. Qualitatively, this behavior of the delay and dispersion (along with numerous other characteristics of fiber gratings) can be nicely explained by an "effective medium picture" developed by Sipe *et al.* [11]. For wavelengths outside the bandgap, the boundaries of the uniform grating (at $z = \pm L/2$) act like abrupt interfaces, thus forming a Fabry-Perot-like cavity. The nulls in the reflection spectrum are analogous to Fabry-Perot resonances-at these frequencies light is trapped inside the cavity for many round-trips, thus experiencing enhanced delay.

2.5 Two modes Coupling in non-uniform grating

In this section, we investigate the properties of non-uniform gratings in which the coupling occurs predominantly between two modes. Most gratings designed for practical applications are not uniform gratings. It has been known for sometime that apodization can reduce the undesirable side-lobes prevalent in uniform-grating spectrum [1], [12], [13]. Chirping the period of a grating enables the dispersive properties of the scattered light to be tailored [1]. One of the applications of a chirped FBG is for dispersion compensation [14].

Direct numerical integration of the coupled mode equations [10] for calculating the reflection and transmission spectrum that results from two mode coupling in non-uniform grating has shown to be straightforward and it uses equation (2.14) and (2.15). The boundary condition for a grating of length L, one generally takes $R(L/2) = 1$ and $S(L/2) = 0$, and then integrates backward from $z = L/2$ to $z = -L/2$, thus obtaining $R(-L/2)$ and $S(-L/2)$.

For modeling apodized gratings by direct numerical integration, we simply use the z-dependent quantities $\sigma_{kj}(z)$ and $\kappa_{kj}(z)$ in the coupled mode equations, which give rise to a $\hat{\sigma}(z)$, that also depends on z. For some apodized grating shapes, we need to truncate the apodization function. For example, FBGs are frequently written by Gaussian beams, and thus have an approximately Gaussian profile of the form

$$\overline{\delta n}_{eff}(z) = \overline{\delta n}_{eff} \exp(-\frac{4\ln 2 z^2}{FWHM^2}) \tag{2.33}$$

where $\overline{\delta n}_{eff}$ is the peak value of the "dc" effective index change and FWHM is the full-width-half-maximum of the grating profile. Typically (2.33) is truncated at several times the FWHM, i.e., we choose L ~ 3FWHM. Another common profile is the "raised-cosine" shape

$$\overline{\delta n}_{eff}(z) = \overline{\delta n}_{eff} \frac{1}{2}[1 + \cos(\frac{\pi z}{FWHM})]. \tag{2.34}$$

This profile is truncated at L=FWHM, where it is identically zero. Many other apodized profiles are of interest as well, such as "flat-top raised cosine."

Chirped FBGs can be modelled using the direct integration technique by simply including a nonzero z-dependent phase term $(\frac{1}{2})d\phi/dz$ in the self coupling coefficient $\hat{\sigma}$ defined in (2.16). In terms of more readily understandable parameters, the phase term for a linear chirp is

$$\frac{1}{2}\frac{d\phi}{dz} = -\frac{4\pi n_{eff} z}{\lambda_D^2}\frac{d\lambda_D}{dz} \tag{2.35}$$

where the "chirp" $d\lambda_D/dz$ is a measure of the rate of change of design wavelength with position in the grating, usually given in units nanometers. Linear chirp can also be specified in terms of a dimensionless "chirp parameter" F [1], given by

$$F = \frac{FWHM^2}{z^2}\phi(z)$$

$$= -4\pi n_{eff}\frac{FWHM^2}{\lambda_D^2}\frac{d\lambda_D}{dz} \tag{2.36}$$

F is a measure of the fractional change in the grating period over the whole length of the grating. It is important to recognize that because chirp is simply incorporated into the coupled-mode equations as a z-dependent term in the self-coupling coefficient $\hat{\sigma}$, its effect is identical to that of a "dc" index variation $\sigma(z)$ with the same z dependence. This equivalence has been used to modify dispersion of gratings without actually varying the grating period [13].

Having described a technique for calculating reflection and transmission spectrum through non-uniform gratings, we now give examples that demonstrate the effects of apodization and chirp on the optical properties of FBGs. To demonstrate the effect of apodization, Figure 2.6 shows the reflection and group delay versus wavelength for grating similar to those described in Figure 2.5, only here the gratings have a Gaussian profile as illustrated in Figure 2.1(b) and described by (2.34). The spectrums are similar except there are no side-lobes on the long-wavelength side and very different side-lobes on the short-wavelength side of the Gaussian spectrum. The short wavelength structure is caused by the non-uniform "dc" index change and has been described in detail elsewhere [4], [11]. The short-wavelength structure lie inside the local band gap ($|\vec{\sigma}| < \kappa$) associated with the wings of the grating and thus are strongly reflected there, but if it lies outside the local band gap near the center of grating where they are only weakly reflected; the wings of the grating thus act like a Fabry-Perot cavity at short wavelength.

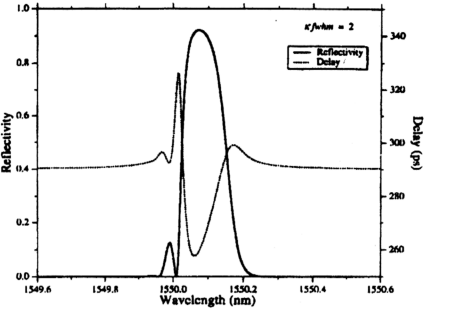

(a) $\kappa L = 2$

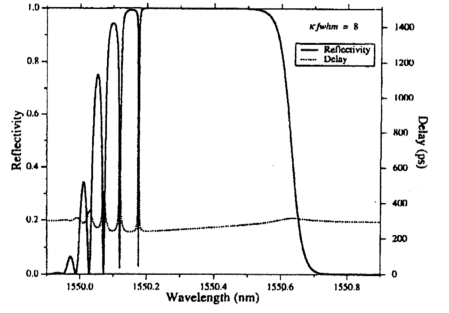

(b) $\kappa L = 8$

Figure 2.6: Calculated reflection spectrum (dotted line) and group delay (solid line) for Gaussian FBG with (a) $\kappa L = 2$ (b) $\kappa L = 8$ [10].

An example of a chirped grating is shown in Figure 2.7. The grating has a "zero-dc" raised-cosine profile with FWHM = 1 cm, $\nu\overline{\delta n}_{eff} = 5x10^{-4}$, and a chirp of $d\lambda_D / dz = -1$ nm/cm. The plot shows group delay calculated from (2.31) (dashed line), and dispersion calculated from (2.32) (solid line) with the associated reflection spectrum (inset). The bandwidth of a similar, unchirped grating estimated from (2.30) is 0.53 nm. A commonly used estimate of dispersion in a linearly chirped grating when variation of grating period along z is the dominant source of chirp is given by

$$d_\rho \sim 100\left(\frac{d\lambda_D}{dz}\right)^{-1} \text{ (ps/nm)} \tag{2.37}$$

where $d\lambda_D / dz$ is in units nm/cm, and we have approximated $2n_{eff} / c \cong 100$ ps/cm. According to (2.37), the grating in Figure 2.7 should exhibit a dispersion of d_ρ=-100 ps/nm and thus a delay of τ_ρ=200 ps between 1549-1551 nm. These simple estimates disagree with the actual values by almost a factor of two, mainly because the effective chirp resulting from apodization is comparable to the grating-period chirp.

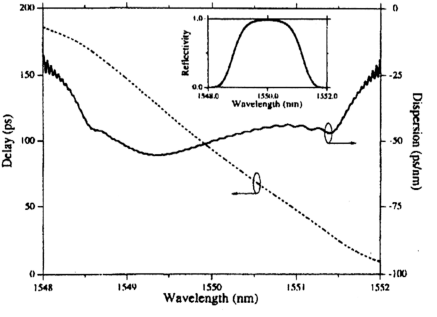

Figure 2.7: Calculated group delay and dispersion of a chirped grating. Inset shows the reflection spectrum [10].

References

1. H. Kogelnik, "Filter response of nonuniform almost-periodic gratings," Bell Syst. Tech. J.,Vol. 55, pp.109-126, 1976.
2. L. A. Weller-Brophy and D. G. Hall, "Analysis of waveguide gratings: Application of Rouard's method," J. Opt. Soc. Amer. A, Vol. 2, pp. 863-871, 1985.
3. M. Yamada and K. Sakuda, "Analysis of almost-periodic distributed feedback slab waveguides via a fundamental matrix approach," Appl. Opt., Vol. 26, pp. 3474-3478, 1987.
4. V. Mizrahi and J. E. Sipe, " Optical properties of photosensitive fiber phase gratings, "J. Lightwave Technol., Vol. 11, pp. 1513-1517, 1993.
5. E. Peral, J. Capmany and J. Marti, "Iterative solution to the Gel'fand-Levitan-Marchenko coupled equations and application to synthesis of fiber gratings," IEEE J. Quantum Electron., 32(12), pp. 2078-2084, 1996.
6. M. Born and E. Wolf, "Principles of Optics," New York: Pergamon, sec. 8.6.1, eq. (8), 1987.
7. A. Yariv, "Coupled-mode theory for guided-wave optics," IEEE J. Quantum Electron., Vol. QE-9, pp.919-933, 1973.
8. H. Kogelnik, "Theory of optical waveguides," inGuided-Wave Optoelectronics, T. Tamir, Ed. New York: Springer-Verlag, 1990.
9. H. Kogelnik, "Coupled wave theory for thick holograms," Bell Syst. Tech. J., 48(9), pp. 2909 – 2947, 1969.
10. T. Erdogan, "Fiber Grating spectra," J. Lightwave Technol., 15(8), pp.1277-1294, 1997.

11. J. E. Sipe, L. Poladian and C. M. deSterke, "Propagation through nonuniform grating structures," J. Opt. Soc. Amer. A, Vol. 11, pp. 1307-1320, 1994.

12. K. O. Hill, "Aperiodic distributed-parameter waveguides for integrated optics," Appl. Opt., Vol. 13, pp. 1853-1856, 1974.

13. B. Malo, S. Theriault, D. C. Johnson, F. Bilodeau, J. Albert and K. O. Hill, "Apodised in-fiber Bragg grating reflectors photoimprinted using a phase mask," Electron. Lett., Vol. 31, pp. 223-225, 1995.

14. F. Ouellette, "Dispersion cancellation using linearly chirped Bragg grating filters in optical waveguides, "Opt. Lett., Vol. 12, pp. 847-849, 1987.